

## The Inclusion of Fetal Bovine Serum in Gelatin/PCL Electrospun Scaffolds Reduces Short-Term Osmotic Stress in HEK 293 Cells Caused by Scaffold Components

Young Hun Kim,<sup>1</sup> Do-Hyung Kim,<sup>2</sup> Junmo Hwang,<sup>1</sup> Hyeng-Soo Kim,<sup>1</sup> Ga Young Lim,<sup>1</sup>  
Zae Young Ryoo,<sup>1</sup> Sang-Un Choi,<sup>3</sup> Sanggyu Lee<sup>1</sup>

<sup>1</sup>School of Life Science and Biotechnology, Kyungpook National University, Daegu, Republic of Korea

<sup>2</sup>School of Physics and Energy Sciences, Kyungpook National University, Daegu, Republic of Korea

<sup>3</sup>Korea Research Institute of Chemical Technology, Daejeon 305-600, Republic of Korea

Correspondence to: S. Lee (E-mail: slee@knu.ac.kr)

**ABSTRACT:** Components of gelatin/polycaprolactone (PCL) electrospun scaffolds are released to surrounding media and cause osmotic changes that adversely affect cell viability and proliferation. In this study, the physiological properties of gelatin/PCL scaffolds were investigated by qRT-PCR and by performing cellular studies on HEK 293 cells. Components released from gelatin/PCL scaffolds were found to induce osmotic stress response in these cells. However, osmotic stress was inhibited by adding fetal bovine serum (FBS) to scaffolds. In addition, focal adhesion related genes were found to be up-regulated in HEK 293 cells on gelatin/PCL/20% FBS scaffolds, and this induced the down-regulations of cell-death related genes. Furthermore, the inclusion of 20% FBS improved the viabilities of HEK 293 cells on gelatin/PCL scaffolds. This study indicates that adding FBS to gelatin/PCL scaffolds improves scaffold bio-affinity. © 2013 Wiley Periodicals, Inc. *J. Appl. Polym. Sci.* 129: 3273–3281, 2013

**KEYWORDS:** biocompatibility; biodegradable; properties and characterization; electrospinning; biomaterials

Received 7 November 2012; accepted 16 January 2013; published online 21 February 2013

**DOI:** 10.1002/app.39052

### INTRODUCTION

Electrospinning provides a powerful means of fabricating scaffolds with structures resembling those of native extracellular matrix. The properties of electrospun scaffolds are controlled by regulating electrospinning conditions, and their bio-affinities are improved by incorporating native extracellular matrix and protein components.<sup>1–4</sup> Gelatin is widely used to fabricate bio-friendly scaffolds and is easily obtained by the hydrolysis of native collagen – a component of extracellular matrix. Scaffolds consisting of gelatin disintegrate under physiological conditions, and therefore, gelatin scaffolds must be cross-linked for biological applications.<sup>5–10</sup> The incorporation of a nontoxic biodegradable polymer into gelatin is commonly used to achieve cross-linking because polymer incorporation provides a simple and efficient means of stabilizing scaffold structurally under physiological conditions.<sup>9,10</sup> In particular, polycaprolactone (PCL) is a non-toxic, bio-applicable polymer that is widely used to cross-link gelatin electrospun scaffolds.<sup>9–12</sup>

Gelatin/PCL electrospun scaffolds have been used for tissue regeneration and various other biological applications, and their

physicochemical properties have been previously described.<sup>9–12</sup> However, information on the bio-affinities of these scaffolds is lacking despite the widespread use of gelatin/PCL scaffolds in biological studies and in the tissue regeneration field.

In this study, the physiological properties of gelatin/PCL scaffolds were investigated *in vitro*, in the hope that this would provide important information about their biological applications.

### EXPERIMENTAL

#### Properties of Electrospun Scaffolds

Information on materials, fabrication conditions, and measurements are provided in Supporting Information Table S1, and details of the classification standard used and scaffold designations are summarized in Table I.

To investigate the chemical structures of scaffolds, Fourier Transform Infrared spectroscopy (FTIR) spectra were obtained using Spectrum GX & AutoImage software (PerkinElmer, USA). The transmittance of each sample was detected at a resolution of 1 cm<sup>-1</sup> between 4000 and 400 cm<sup>-1</sup>.

Additional Supporting Information may be found in the online version of this article.

© 2013 Wiley Periodicals, Inc.

**Table I.** Classification Criteria and Names of the Electrospun Scaffolds

Name of scaffold	Components of solution		
	Solute <sup>a</sup> (each w/v%)	Solvent <sup>b</sup> (v/v%)	FBS content <sup>c</sup> (v/v%)
AF0	Gelatin type A 10%, PCL 10%	50%	N/A
AF1	Gelatin type A 10%, PCL 10%		10%
AF2	Gelatin type A 10%, PCL 10%		20%
BF0	Gelatin type B 10%, PCL 10%		N/A
BF1	Gelatin type B 10%, PCL 10%		10%
BF2	Gelatin type B 10%, PCL 10%		20%

<sup>a</sup>Weight of each solute (g)/volume of solvent (mL).

<sup>b</sup>Volume of TFE (mL)/volume of (TFE+ddH<sub>2</sub>O) (mL).

<sup>c</sup>Volume of FBS (mL)/volume of total solution (mL).

Morphologies of scaffolds were analyzed using a field emission scanning electron microscope (FE-SEM, S-4300 & EDX-350 HITACHI). The thermal analysis of gelatin/PCL scaffolds was performed by Thermogravimetry/Differential Thermal Analysis (TG/DTA, SDT Q600 V20.9 Build 20, TA Instruments) and using a differential scanning calorimeter (DSC; Q2000 V24.4 Build 116; TA Instruments). The analysis conditions used for TG/DTA and DSC were as follows. TG/DTA was performed under nitrogen and the temperature was increased from 10°C to 800°C at 10°C/min, and for DSC, samples were heated from 10°C to 150°C at 10°C/min.

Scaffold swelling analysis was performed as previously described by Meng et al.<sup>13</sup> Swelling ratios (%) were calculated using  $(W - W_0)/W_0 \times 100\%$ , where  $W_0$  is the initial weight and  $W$  is the wet scaffold weight.<sup>13</sup>

#### Bio-Effects of Components Released from Gelatin/PCL Scaffolds

Scaffolds were sterilized using 70% ethanol for 20 min under UV light, and the ethanol was removed using DPBS. Scaffolds were then incubated with 100-fold of cell growth media (DMEM) containing 10% FBS [volume of media (mL)/weight of scaffold (g)] for 1 day in a 5% CO<sub>2</sub> humidified incubator at 37°C without cells. To remove scaffold debris, media (referred to as “conditioned media”) were passed through a 0.22- $\mu$ m syringe filter (Millipore, USA).

The effects of components released from scaffolds on cell viability were examined using human embryonic kidney 293 (HEK 293) cells. Cells ( $2 \times 10^5$ ) were seeded in a 96-well plate in 0.1 mL fresh or conditioned media. Cell viabilities and proliferation rates were measured using CCK-8. The proliferation curves of HEK 293 cells were obtained by exponential trendline analysis, but the proliferation curve of cells under starvation conditions was analyzed using log trendline analysis. The reliabilities of results were determined using  $R^2$  values.

Changes in gene expressions induced by components released from scaffolds were analyzed by quantitative RT-PCR (qRT-PCR). HEK 293 cells ( $2 \times 10^6$ ) were seeded in 6-well plates and incubated for 24 h in cell growth medium (DMEM) containing 10% FBS. The medium was then replaced with 1ml conditioned media. The process is explained in detail in the section that addresses qRT-PCR below.

#### Bio-Affinities of Gelatin/PCL Scaffolds

HEK 293 cells and circular scaffolds (18-mm diameter) were used to analyze scaffold bio-affinities. The viabilities of HEK 293 cells on scaffolds were analyzed using CCK-8. Briefly, HEK 293 cells ( $2 \times 10^4$ ) were seeded on scaffolds and 18-mm culture dishes, and incubated in cell growth medium (DMEM) containing 10% FBS. Scaffolds and plates were then washed with DPBS, and attached cells were harvested using 0.25% Trypsin-EDTA. Densities of harvested cells were calculated using CCK-8. qRT-PCR was performed to investigate the gene expression patterns of HEK 293 cells on electrospun scaffolds.

#### Quantitative RT-PCR

For qRT-PCR analysis, RNA was purified using RNeasy Mini kits (Qiagen). Briefly, RNA (3  $\mu$ g) was reverse-transcribed to cDNA using M-MLV Reverse Transcriptase (Invitrogen), and gene expression levels were measured using SYBR green reagents (TaKaRa) using the primer sets detailed in Supporting Information Table S2. Reactions were performed in an ABI StepOne Plus (Applied Biosystems), and results were analyzed using StepOne software (Applied Biosystems).

#### Data Analysis and Statistics

The results are presented as mean  $\pm$  standard deviation. Statistical analysis were performed by Student's  $t$ -test, with significance reported when  $P < 0.05$ .

## RESULTS AND DISCUSSION

### Morphological Properties

Morphologically scaffolds were composed of smooth nanofibers (Figure 1). However, variations in structure were observed under physiological conditions, such as, the spreading of the nanofibers (X day incubated sections in Figure 1). Furthermore, the diameter distributions of gelatin type B scaffolds were narrower than those of gelatin type A scaffolds produced under the same conditions (Supporting Information Figure S1). Comparisons of gelatin/PCL scaffolds with or without FBS revealed that fiber diameters were reduced by FBS.

### Physicochemical Properties of Scaffolds

TG/DTA was used to examine the thermal properties of gelatin/PCL scaffolds (Figure 2). Weight loss occurred at temperatures of  $<100^\circ\text{C}$  for all samples (except PCL) due to the evaporation of water absorbed by the gelatin. In the temperature range between  $250^\circ\text{C}$  and  $450^\circ\text{C}$ , a large mass loss was observed for all samples. Differences in thermal gravimetric results reflected the thermal characteristics of gelatin powder, PCL, and gelatin/PCL.<sup>12,14,15</sup> Gelatin and PCL powders have specific DTGA peaks (Supporting Information Figure S2). More specifically, gelatin powders have two peaks at  $<100^\circ\text{C}$  and  $\sim 320^\circ\text{C}$ , whereas PCL powders have two peaks at  $\sim 320^\circ\text{C}$  and  $\sim 400^\circ\text{C}$ . These gelatin and PCL peaks were also observed for gelatin/PCL scaffolds.

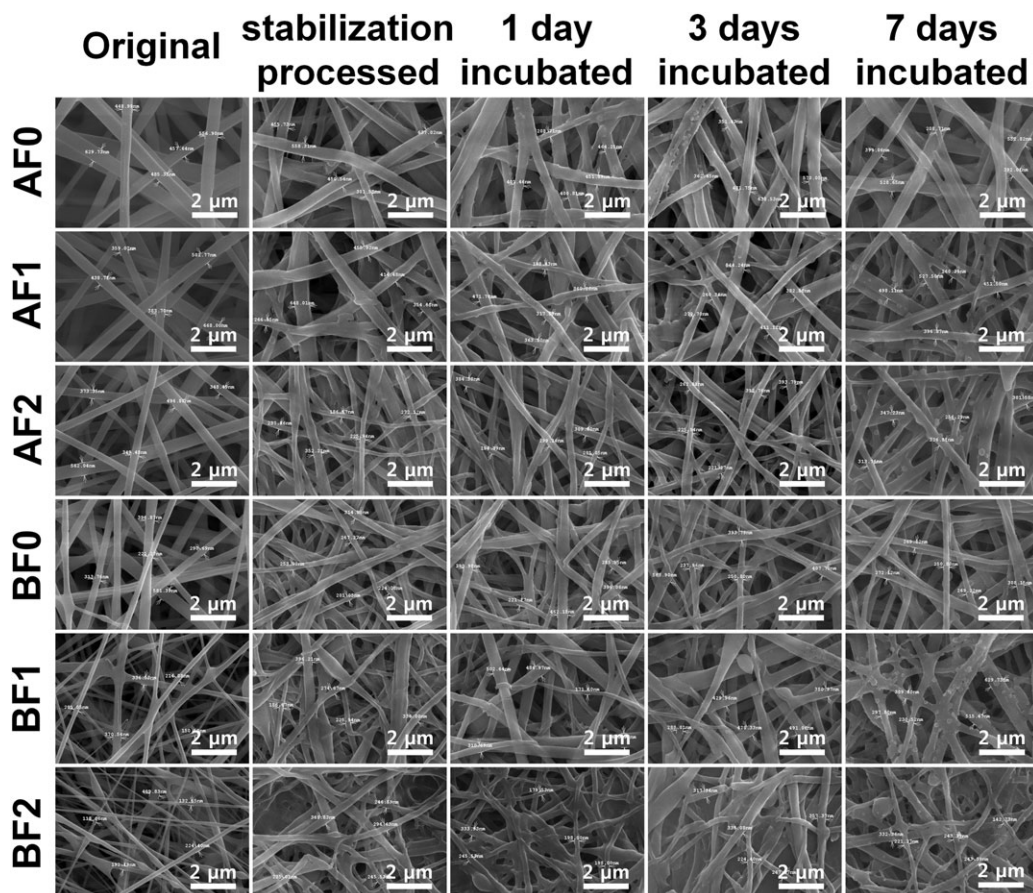


**Figure 1.** Morphologies of gelatin/PCL scaffolds by FE-SEM. “X-day incubated” indicates that stabilization processed scaffold was incubated for X days in biological fluid at 37°C under 5% CO<sub>2</sub>.

Residual masses were ~19%, 0%, and 11% for gelatin powder, PCL, and the gelatin/PCL scaffolds, respectively (Figure 2). These results indicate that the thermal stabilities of scaffolds were improved by mixing gelatin and PCL.<sup>12</sup>

The FTIR spectra of gelatin/PCL scaffolds exhibited specific peaks of gelatin powder, PCL, and FBS (Figure 3 and Supporting Information for detail information). In particular, in the FTIR spectra of scaffolds, the intensity of the ~682 cm<sup>-1</sup> (a FBS specific peak due to the overlapping of amides IV, V, and

VI) increased in proportion to FBS content in gelatin/PCL scaffolds. The results obtained showed that the gelatin/PCL/FBS scaffolds contained the intended ratio of FBS.

Although the thermal stabilities of scaffolds were improved by mixing gelatin and PCL, thermal variations were observed at low temperatures. Therefore, we examined the thermal properties of all scaffolds at low temperatures by DSC (Table II and Supporting Information Figure S3). The results obtained showed that the enthalpies of gelatin/PCL scaffolds were lower

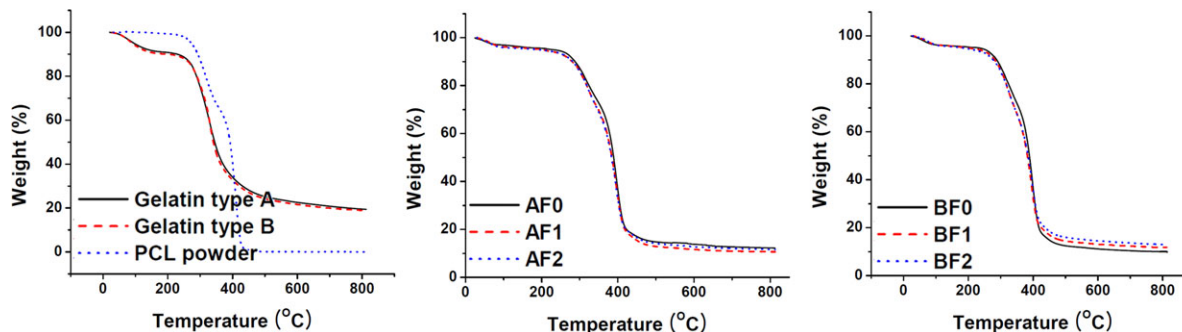


**Figure 2.** Thermal properties of scaffold components and scaffolds as determined by TG/DTA. [Color figure can be viewed in the online issue, which is available at [wileyonlinelibrary.com](http://wileyonlinelibrary.com).]

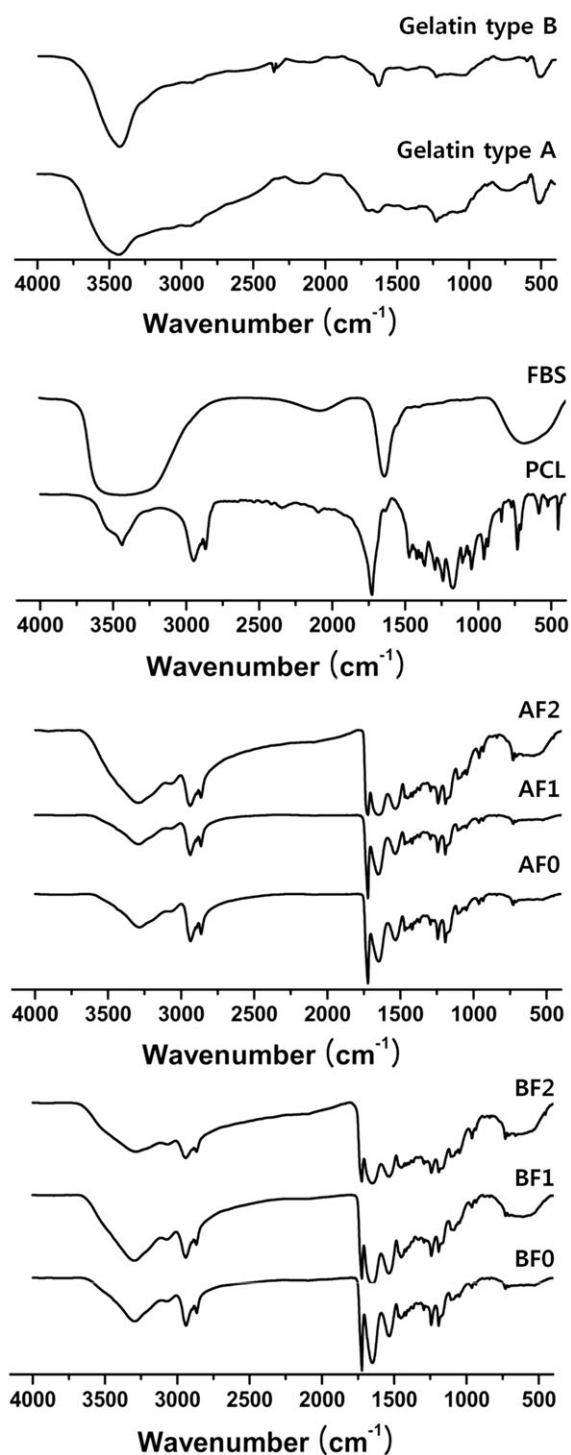


Figure 3. FTIR results of components and scaffolds.

than that of PCL powder, indicating that the gelatin positively interacted with the PCL.<sup>16</sup> Furthermore, the enthalpies of scaffolds were reduced by adding FBS. It suggests that FBS improves scaffold thermal stability and molecular interaction between scaffold components. Despite the enthalpy variations observed, scaffold denaturation onset and peak temperatures were higher than 37°C (Table II). It indicates that all scaffolds were stable at physiological temperatures.

Table II. Thermal Properties of Scaffolds and Powders

	Onset $T_D^a$ (°C)	Peak $T_D^a$ (°C)	Enthalpy (J/g)
AF0	52.39	55.50	46.76
AF1	51.77	54.82	36.88
AF2	52.01	55.52	38.30
BF0	52.11	56.05	43.06
BF1	52.08	56.35	38.35
BF2	51.37	55.34	30.64
Gelatin type A powder	N/A	N/A	N/A
Gelatin type B powder	N/A	N/A	N/A
PCL powder	59.65	64.43	94.51

<sup>a</sup>Denaturation temperatures ( $T_D$ ).

### Hydrophilicity and Morphological Stability Under Physiological Condition

The hydrophilicities of scaffolds were used to estimate their bio-affinities,<sup>13,17</sup> and were determined by swelling analysis. Swelling rates decreased on increasing FBS content (Figure 4), presumably due to the hydrophobic components of FBS. Nevertheless, swelling rates remained above 200%.

The maintenance of a nanofibrous structure under physiological condition also importantly determines bio-affinity scaffolds.<sup>18</sup> Figure 1 shows that some morphological changes of nanofibers were observed under physiological condition. Despite these changes, the nanofiber structure was maintained (Figure 1). These results indicate that the hydrophilic- and structural properties of gelatin/PCL scaffolds are commensurate with requirements for biological applications.

### Short-Term Osmotic Stress Induced by Components Released from Scaffolds in HEK 293 Cells

Bio-degradable electrospun scaffolds decompose in physiological environments, which means that scaffold components are

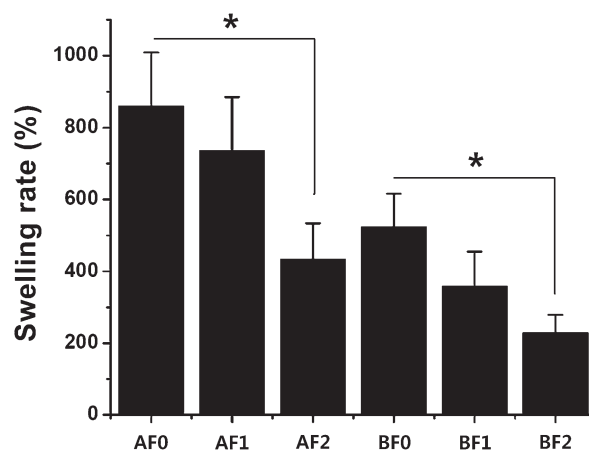
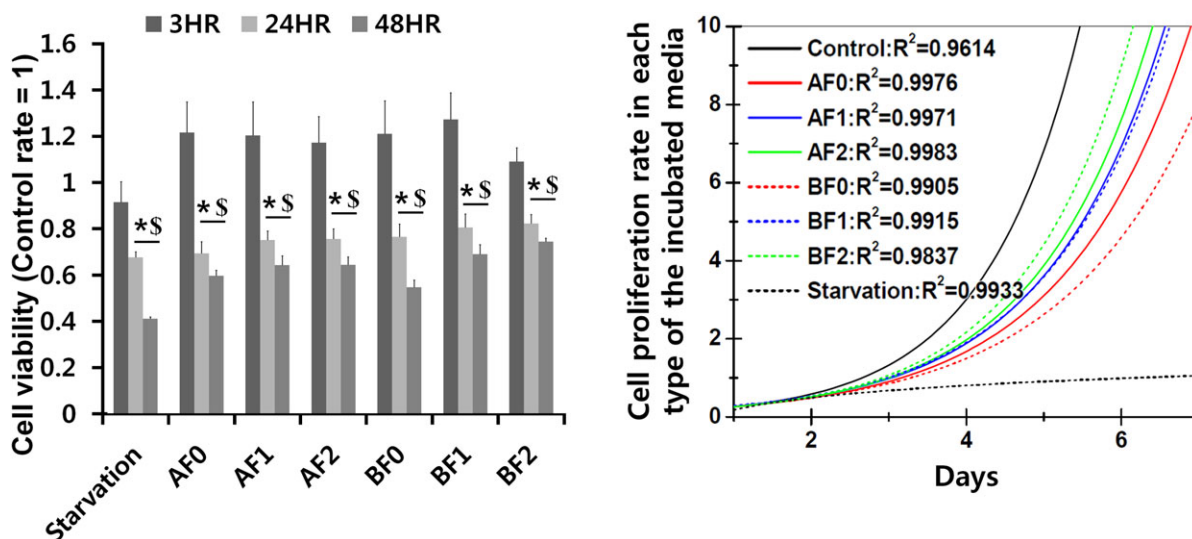


Figure 4. Swelling analysis results (\* $P < 0.05$ ).



**Figure 5.** The viabilities and proliferations of HEK 293 cells in different types of conditioned media ( $n = 3$ ,  $*P < 0.05$  for 3 h vs. 24 h and 48 h,  $^{\$}P < 0.05$  for the control vs. the experimental group). [Color figure can be viewed in the online issue, which is available at [wileyonlinelibrary.com](http://wileyonlinelibrary.com).]

released.<sup>14,19,20</sup> The morphological change of gelatin/PCL scaffold in physiological condition is occurred by swelling of scaffold, which induces the decomposition of gelatin/PCL scaffold.<sup>21</sup> The morphological variations of scaffolds were observed by the swelling (Figure 1). In the case of gelatin/PCL scaffolds, their components were released (Supporting Information Figure S4).

*In vitro*, these components accumulate in cell growth media and change its osmotic pressure, which adversely affects normal cell growth, as was observed in the present study for HEK 293 cells (Figures 5 and 6). However, interestingly, the proliferation rates of HEK 293 cells in conditioned media were increased by adding FBS to gelatin/PCL scaffolds (Figure 5). Furthermore,

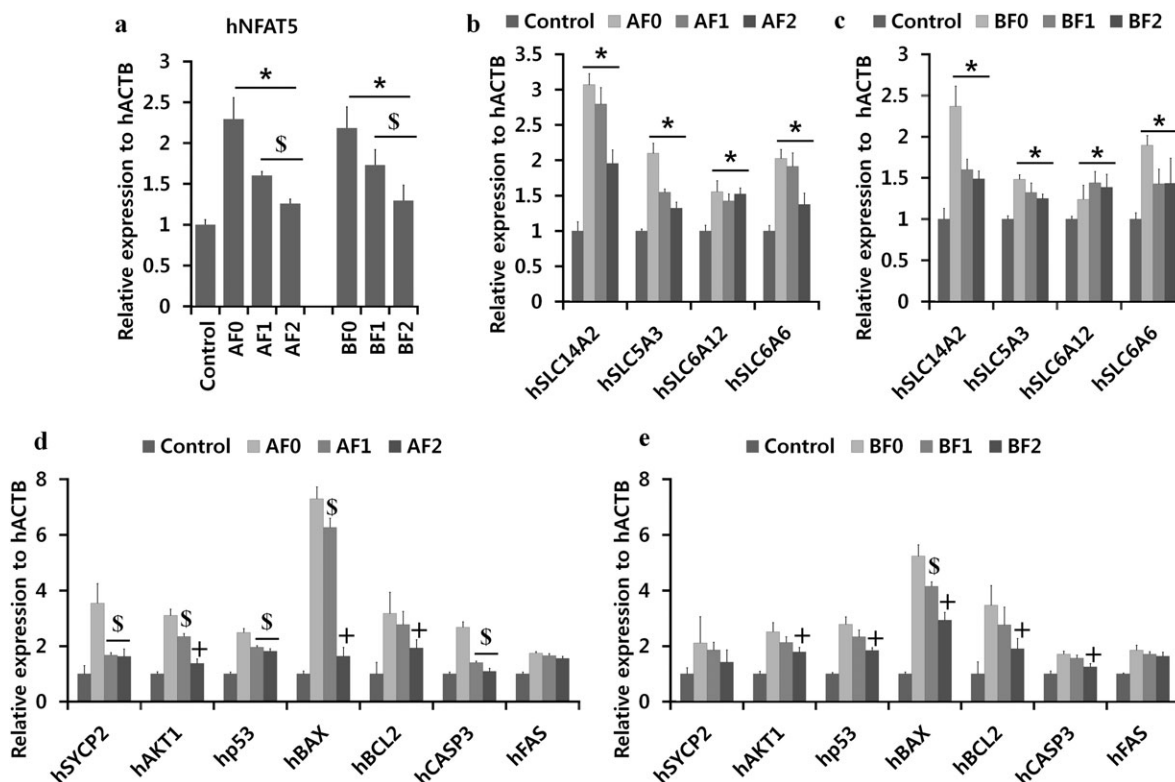


**Figure 6.** Changes in the gene expressions of HEK 293 cells in 1-mL of conditioned media from different scaffolds. Cells were cultured for 24 h ( $n = 9$ ,  $*P < 0.05$  for the control (ratio = 1) vs. the experimental group,  $^{\$}P < 0.05$  for F0 vs. F1 and F2,  $^{+}P < 0.05$  for F1 vs. F2). (a) Expression level of *hNFAT5*. (b, c) Expression patterns of compatible osmolyte and urea transporter genes. (e, f) Expression levels of cell death-related genes.

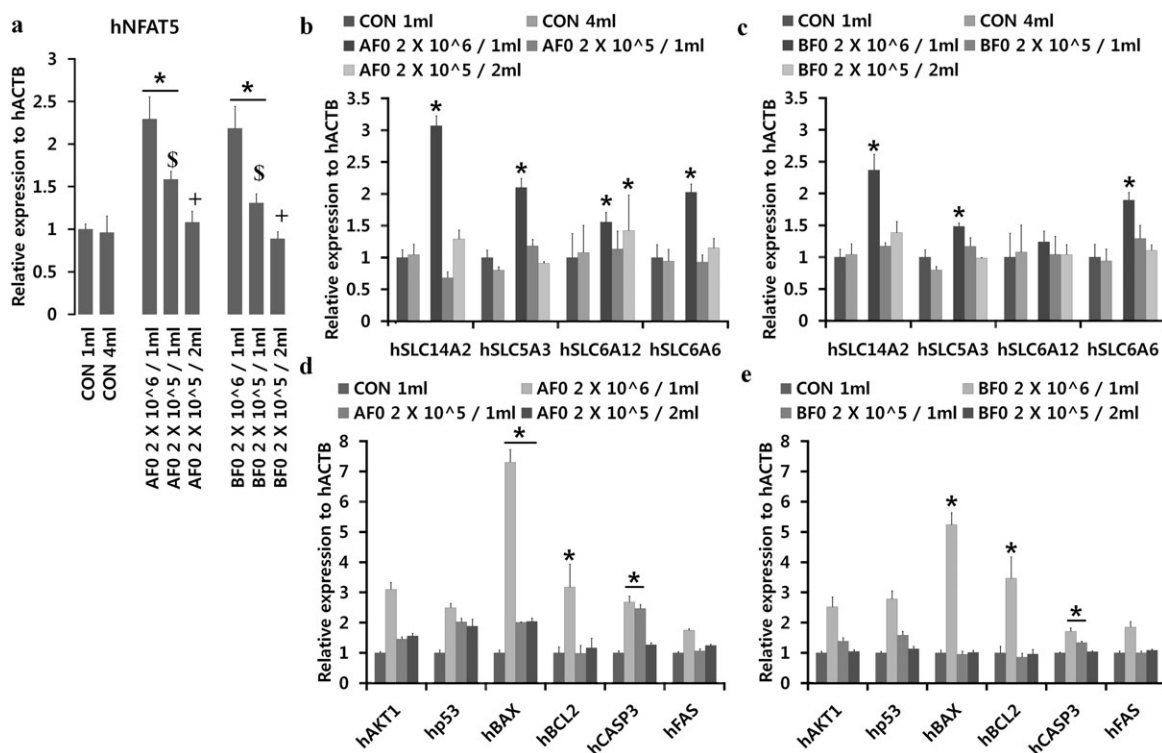


**Figure 7.** Relationship between HEK 293 cell density in conditioned media containing released components from gelatin/PCL scaffolds and osmotic response ( $n = 9$ ,  $*P < 0.05$  for the control (ratio = 1) vs. the experimental group,  $^{\$}P < 0.05$  for F0 vs. F1 and F2,  $^{+}P < 0.05$  for F1 vs. F2). HEK 293 cells were cultured in conditioned media for 24 h. (a) Expression level of *hNFAT5*. (b, c) Expression patterns of compatible osmolyte and urea transporter genes. (d, e) Changes in the expressions of cell death related genes.

changes in the expression levels of osmotic stress-, cell death-, and cell cycle genes were gradually reduced by adding FBS (Figure 6 and Supporting Information Figure S5).

In addition, changes in the expression of *hNFAT5* (*TonEBB*, an osmotic stress marker gene) and in those of cell death related genes were found to be significantly reduced by decreasing cell density in conditioned media (Figure 7). This phenomenon is explained by a regulatory volume increase (RVI) that is a specific cellular response in hypertonic environments designed to maintain cellular homeostasis.<sup>22,23</sup> The transcription factor *hNFAT5* is a central regulator of the osmoprotective pathway,<sup>22–25</sup> and when activated by hypertonicity, *hNFAT5* stimulates the transcriptions of ion transporter genes, which in turn increases the intracellular concentrations of potassium, sodium, and chloride ions, and induces water influx into cells that prevents cell shrinkage.<sup>22,23</sup> However, abnormal increases in intracellular ionic concentrations cause cellular damage, such as, DNA double-strand breaks,<sup>26</sup> and thus, abnormally elevated intracellular ions must be removed. These ions are discharged from cell body by exchange of amino acids and compatible osmolytes, such as, betain, taurine, myo-inositol, and others.<sup>22,23,27,28</sup>

Osmotic response can be classified as “early responses” (milliseconds to minutes, *hNFAT5* up-regulated, ions transport) and “later responses” [exchange of amino acids (hour) and compatible osmolytes (day)].<sup>22</sup> In this study, gene expression patterns were analyzed after 1 day of treatment with conditioned media,

which is known as the “later responses” in the osmo-protective pathway.<sup>22</sup> Therefore, expression levels of *hNFAT5* and compatible osmolyte transporter genes can reflect completeness of osmo-protection response.

The expressions of osmotic response genes were found to be dependent on cell density in conditioned media (Figure 7). Compatible osmolyte transporter genes, such as, *hSLC6A12* (sodium chloride-betaine cotransporter), *hSLC6A6* (taurine transporter), *hSLC5A3* (sodium / myo-inositol cotransporter), *hSLC14A2* (urea transporter), and *hNFAT5* were found to be expressionally up-regulated at high cell densities. However, changes in the expression levels of these genes were reduced by lowering cell density in conditioned media (Figure 7). These observations suggest that the osmo-protective mechanism was not fully active at high cell densities in conditioned media. Compatible osmolytes and amino acids are important components of osmo-protection and their levels in media were maintained at constant levels. However, when cell densities were high, presumably, the amounts of compatible osmolytes and amino acids in conditioned media were not sufficient to sustain osmo-protection. On the other hand, at low cell densities, levels of compatible osmolytes and amino acids in same volume of conditioned media were relatively higher than at high cell densities. Therefore, the osmo-protective mechanism functions normally at low cell densities. When full adaptation of RVI is prevented by a shortage of compatible osmolytes and amino acids, cells

undergo apoptosis.<sup>28,29</sup> In the present study, in conditioned medium, changes in the expression levels of cell death genes were reduced by decreasing cell density. In particular, the expression of *hCASP3*, a major marker of cell death, was unchanged at low cell densities [Figure 7(d,e)].

Taken together, the components released from gelatin/PCL scaffolds to media appear to cause short-term osmotic stress, and furthermore, when full adaptation of RVI is blocked by deprivation of compatible osmolytes and amino acids, abnormal cellular responses occur, such as, the abnormal expressions of cell death and cell cycle related genes.<sup>22–26,28–30</sup>

### Biocompatibilities of Gelatin/PCL/FBS Scaffolds

FBS contains several important biological molecules and growth supporting factors that affect the properties of cell culture media, such as, viscosity, osmolality, buffering capacity, and diffusion rate.<sup>31</sup> In the case of gelatin/PCL scaffolds containing FBS, amounts of FBS in conditioned media increased in proportion to its levels in scaffolds. Higher levels of FBS in conditioned media increases amino acid levels and the levels of compatible osmolytes required for osmo-protection. Therefore, the expression levels of osmotic stress genes and cell death related genes in conditioned media reduced in proportion to FBS content in gelatin/PCL scaffolds (Figure 6). It is known that when full adaptation of RVI is blocked, cells adopt a shrunken morphology.<sup>22,23</sup> However, the morphology of HEK 293 cells in the conditioned media of gelatin/PCL/20% FBS scaffold was not significantly changed (Supporting Information Figure S6). These results indicate that the addition of FBS to gelatin/PCL scaffolds

improves scaffold bio-affinity by blocking osmotic stress induced by released components.

In the present study, osmotic stress response was significantly reduced in conditioned media from gelatin/PCL/20% FBS scaffolds (Figure 6). Therefore, we examined HEK 293 response on gelatin/PCL/20% FBS scaffolds. No significant change in morphology was observed (Figure 8). However, the viabilities of HEK 293 cells on scaffolds containing 20% FBS were lower than their viabilities on culture dishes for 3 days [Figure 9(a)]. Cell adhesion and proliferation on polymer surfaces are affected by surface hydrophilicity,<sup>32,33</sup> and although biodegradable polymer was added to improve the physicochemical and thermal stabilities of gelatin electrospun scaffolds, hydrophilicities were reduced by increasing polymer content.<sup>13,34</sup> The hydrophilicities of gelatin/PCL scaffolds were reduced by increasing FBS content, as determined by swelling analysis (Figure 4). Additionally, it is known that cell attachment to scaffolds is known to be poor.<sup>17</sup> Therefore, reduced cell viability on gelatin/PCL/20% FBS scaffolds for 3 days was caused by reduced cell attachment on the scaffolds. However, on culture 5 days, cell viabilities on scaffolds were similar to control levels [Figure 9(a)], which shows that HEK 293 cell growth on gelatin/PCL/20% FBS scaffolds improved.

Responses of HEK 293 cells on gelatin/PCL/20% FBS scaffolds were analyzed by qRT-PCR. It was found that these cells were not influenced by the osmotic stress caused by released components [Figure 9(b)]. Gelatin/PCL scaffolds are known to affect focal adhesion signaling,<sup>35</sup> and in the present study, focal adhesion related genes were found to be up-regulated on gelatin/

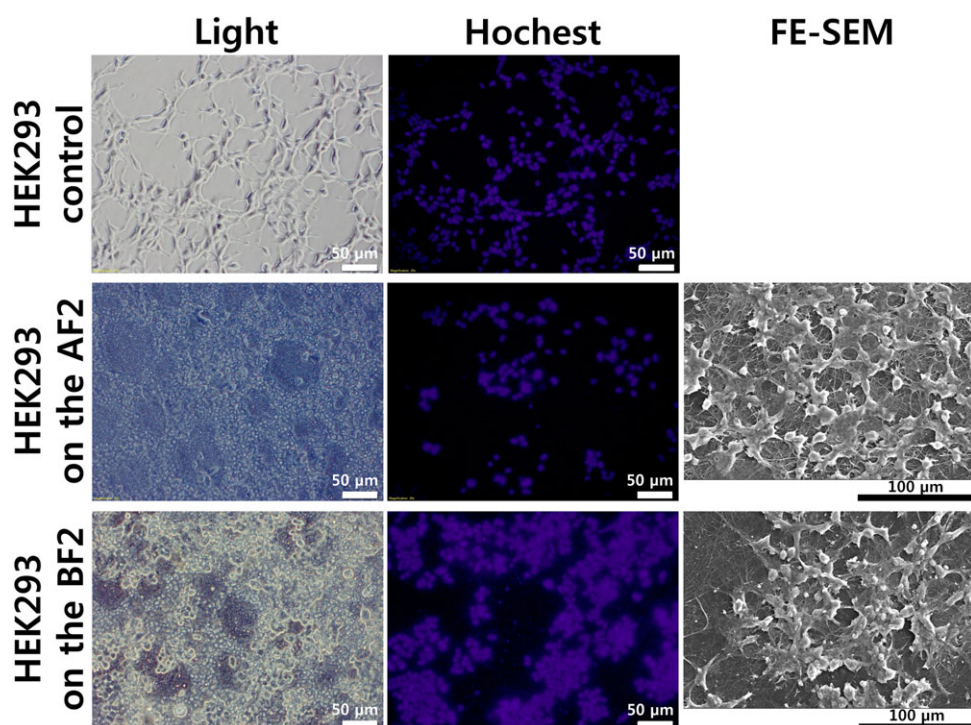


**Figure 8.** Morphologies of HEK 293 cells on two types of gelatin/PCL/20% FBS scaffolds. HEK 293 cells were cultured for 5 days. [Color figure can be viewed in the online issue, which is available at [wileyonlinelibrary.com](http://wileyonlinelibrary.com).]

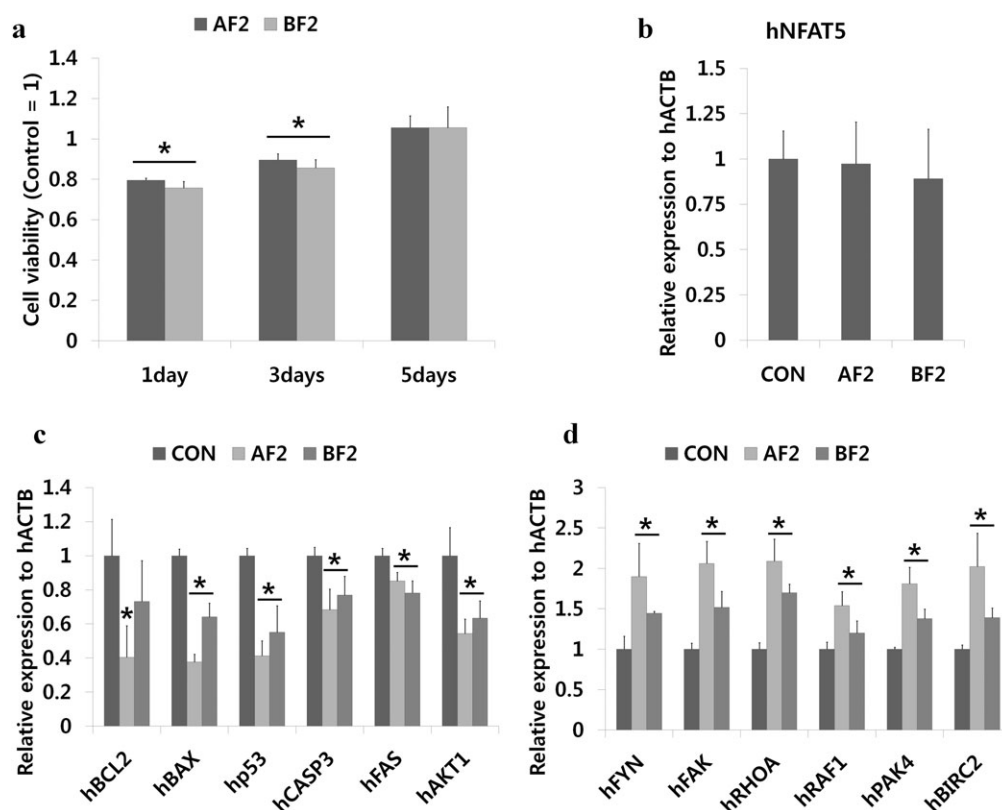


**Figure 9.** Effects of gelatin/PCL/20% FBS electrospun scaffolds on attached HEK 293 cells. Gene expression patterns of HEK 293 cells cultured for 24 h were determined by qRT-PCR ( $n = 9$ ,  $*P < 0.05$  for control vs. the experimental group). (a) Cell viabilities on scaffolds, (b) Gene expressions of *hNFAT5*, (c) Expressions of cell death-related genes, and (d) Variations in the expressions of focal adhesion genes.

PCL/20% FBS scaffolds [Figure 9(d)]. Furthermore, focal adhesion signaling is known to be closely related to cell death signaling,<sup>36–38</sup> for example, *hBIRC2* is a member of the inhibitor of apoptosis family and inhibits apoptosis by interfering with the activation of caspase-3.<sup>39,40</sup> In this study, the expression level of *hCASP3* was decreased, and the other cell death related genes were also down-regulated [Figure 9(c)]. Therefore, the focal adhesion signaling of HEK 293 cells was increased on gelatin/PCL/20% FBS scaffolds, which induced the down-regulations of cell death related genes. These results indicate that the changes in the gene expressions of HEK 293 cells on scaffolds containing 20% FBS promote cell viability.

#### Relationship Between Gelatin Type and Scaffold Biocompatibility

Differences between gelatin type A and type B scaffolds were observed by performing physicochemical analysis and cellular studies. However, neither the morphology nor viability of HEK 293 cells on gelatin/PCL/20% FBS scaffolds was found to be significantly altered by gelatin types. Cellular responses on gelatin/PCL scaffolds are only slightly modified by gelatin type. Accordingly, gelatin type was not found to be important in terms of determining gelatin/PCL/20% FBS scaffold bio-affinity.

#### CONCLUSIONS

Components of gelatin/PCL scaffolds are released to surround media *in vitro*, and these released components can induce

short-term osmotic stress response in cells and detrimentally affect cell growth. The addition of FBS to gelatin/PCL scaffolds inhibited the osmotic stress induced by conditioned media by increasing amino acid and compatible osmolyte levels in conditioned media. In addition, focal adhesion signaling of HEK 293 cells on gelatin/PCL/20% FBS scaffolds was up-regulated, which induced down-regulations of cell death related genes. Thus, these changes in gene expression shown by HEK 293 cells on gelatin/PCL/20% FBS scaffolds, improved cell viability. These results indicate that adding FBS to gelatin/PCL scaffolds improves bio-compatibility by up-regulating focal adhesion related genes and by reducing the osmotic stress induced by the release of scaffold components.

#### ACKNOWLEDGMENTS

This research was supported by Kyungpook National University Research Fund, 2012 and a grant of the Technology Innovation Program (10038744) of Korea Evaluation Institute of Industrial Technology (KEIT) funded by MKE, Republic of Korea.

#### REFERENCES

- Kong, C. S.; Lee, T. H.; Lee, S. H.; Kim, H. S. *J. Mater. Sci.* **2007**, *42*, 8106.
- Teo, W. E.; Ramakrishna, S. *Nanotechnology* **2006**, *17*, R89.
- Han, D.; Gouma, P. I. *Nanomedicine* **2006**, *2*, 37.



4. Hong, J. K.; Madihally, S. V. *Tissue Eng. Part B: Rev.* **2011**, *17*, 125.
5. Cao, M. Y.; Chen, Z. J.; Tu, K. H.; Wang, L. Q.; Jiang, H. L. *Acta Polym. Sin.* **2009**, 1157.
6. Zhang, Y. Z.; Venugopal, J.; Huang, Z. M.; Lim, C. T.; Ramakrishna, S. *Polymer* **2006**, *47*, 2911.
7. Sisson, K.; Zhang, C.; Farach-Carson, M. C.; Chase, D. B.; Rabolt, J. F. *Biomacromolecules* **2009**, *10*, 1675.
8. Zhang, K. H.; Qian, Y. F.; Wang, H. S.; Fan, L. P.; Huang, C.; Yin, A. L.; Mo, X. M. *J. Biomed. Mater. Res. A* **2010**, *95*, 870.
9. Chong, E. J.; Phan, T. T.; Lim, I. J.; Zhang, Y. Z.; Bay, B. H.; Ramakrishna, S.; Lim, C. T. *Acta Biomater.* **2007**, *3*, 321.
10. Zhang, Y.; Ouyang, H.; Lim, C. T.; Ramakrishna, S.; Huang, Z. M. *J. Biomed. Mater. Res. B: Appl. Biomater.* **2005**, *72*, 156.
11. Heydarkhan-Hagvall, S.; Schenke-Layland, K.; Dhanasopon, A. P.; Rofail, F.; Smith, H.; Wu, B. M.; Shemin, R.; Beygui, R. E.; MacLellan, W. R. *Biomaterials* **2008**, *29*, 2907.
12. Chiono, V.; Ciardelli, G.; Vozzi, G.; Cortez, J.; Barbani, N.; Gentile, P.; Giusti, P. *Eng. Life Sci.* **2008**, *8*, 226.
13. Meng, Z. X.; Wang, Y. S.; Ma, C.; Zheng, W.; Li, L.; Zheng, Y. F. *Mater. Sci. Eng. C: Mater. Biol. Appl.* **2010**, *30*, 1204.
14. Prabu, P.; Dharmaraj, N.; Aryal, S.; Lee, B. M.; Ramesh, V.; Kim, H. Y. *J. Biomed. Mater. Res. A* **2006**, *79*, 153.
15. Kim, S. E.; Heo, D. N.; Lee, J. B.; Kim, J. R.; Park, S. H.; Jeon, S.; Kwon, I. K. *Biomed. Mater.* **2009**, *4*.
16. Hajiali, H.; Shahgasempour, S.; Naimi-Jamal, M. R.; Peirovi, H. *Int. J. Nanomed.* **2011**, *6*, 2133.
17. Alvarez-Perez, M. A.; Guarino, V.; Cirillo, V.; Ambrosio, L. *Biomacromolecules* **2010**, *11*, 2238.
18. Agarwal, S.; Wendorff, J. H.; Greiner, A. *Polymer* **2008**, *49*, 5603.
19. Luong-Van, E.; Grondahl, L.; Chua, K. N.; Leong, K. W.; Nurcombe, V.; Cool, S. M. *Biomaterials* **2006**, *27*, 2042.
20. Wang, H.; Feng, Y.; Zhao, H.; Lu, J.; Guo, J.; Behl, M.; Lendlein, A. *J. Control. Release* **2011**, *152* (Suppl 1), e28.
21. Wu, S. C.; Chang, W. H.; Dong, G. C.; Chen, K. Y.; Chen, Y. S.; Yao, C. H. *J. Bioactive Compatible Polym.* **2011**, *26*, 565.
22. Alfieri, R. R.; Petronini, P. G. *Pflugers Archiv-Eur. J. Physiol.* **2007**, *454*, 173.
23. Burg, M. B.; Ferraris, J. D.; Dmitrieva, N. I. *Physiol. Rev.* **2007**, *87*, 1441.
24. Do Lee, S.; Choi, S. Y.; Lim, S. W.; Lamitina, S. T.; Ho, S. N.; Go, W. Y.; Kwon, H. M. *Am. J. Physiol.-Renal Physiol.* **2011**, *300*, F707.
25. Lee, J. H.; Kim, M.; Im, Y. S.; Choi, W.; Byeon, S. H.; Lee, H. K. *Invest. Ophthalmol. Vis. Sci.* **2008**, *49*, 1827.
26. Kultz, D.; Chakravarty, D. *Proc. Natl. Acad. Sci. USA* **2001**, *98*, 1999.
27. Burg, M. B.; Kwon, E. D.; Kultz, D. *Ann. Rev. Physiol.* **1997**, *59*, 437.
28. Alfieri, R. R.; Cavazzoni, A.; Petronini, P. G.; Bonelli, M. A.; Caccamo, A. E.; Borghetti, A. F.; Wheeler, K. P. *J. Physiol. Lond.* **2002**, *540*, 499.
29. Petronini, P. G.; Alfieri, R. R.; Losio, M. N.; Caccamo, A. E.; Cavazzoni, A.; Bonelli, M. A.; Borghetti, A. F.; Wheeler, K. P. *Am. J. Physiol.-Regulatory Integrative Compar. Physiol.* **2000**, *279*, R1580.
30. Criollo, A.; Galluzzi, L.; Maiuri, M. C.; Tasdemir, E.; Lavandro, S.; Kroemer, G. *Apoptosis* **2007**, *12*, 3.
31. Zheng, X. Y.; Baker, H.; Hancock, W. S.; Fawaz, F.; McCaman, M.; Pungor, E. *Biotechnol. Prog.* **2006**, *22*, 1294.
32. Lee, S. J.; Lim, G. J.; Lee, J. W.; Atala, A.; Yoo, J. J. *Biomaterials* **2006**, *27*, 3466.
33. Zhu, X. L.; Cui, W. G.; Li, X. H.; Jin, Y. *Biomacromolecules* **2008**, *9*, 1795.
34. Zhang, Y. Z.; Ouyang, H. W.; Lim, C. T.; Ramakrishna, S.; Huang, Z. M. *J. Biomed. Mater. Res. B: Appl. Biomater.* **2005**, *72*, 156.
35. Sisson, K.; Zhang, C.; Farach-Carson, M. C.; Chase, D. B.; Rabolt, J. F. *J. Biomed. Mater. Res. A* **2010**, *94*, 1312.
36. Aplin, A. E.; Howe, A.; Alahari, S. K.; Juliani, R. L. *Pharmacol. Rev.* **1998**, *50*, 197.
37. Kurenova, E.; Xu, L. H.; Yang, X. H.; Baldwin, A. S.; Craven, R. J.; Hanks, S. K.; Liu, Z. G.; Cance, W. G. *Mol. Cell. Biol.* **2004**, *24*, 4361.
38. Zhan, M.; Zhao, H.; Han, Z. C. *Histol. Histopathol.* **2004**, *19*, 973.
39. Deveraux, Q. L.; Roy, N.; Stennicke, H. R.; Van Arsdale, T.; Zhou, Q.; Srinivasula, S. M.; Alnemri, E. S.; Salvesen, G. S.; Reed, J. C. *EMBO J.* **1998**, *17*, 2215.
40. Burke, S. P.; Smith, L.; Smith, J. B. *J. Biol. Chem.* **2010**, *285*, 30061.